Cell Death and Differentiation (2011), 1–11

www.nature.com/cdd

Prelamin A-mediated recruitment of SUN1 to the nuclear envelope directs nuclear positioning in human muscle

E Mattioli[1], M Columbaro[2], C Capanni[1], NM Maraldi[2], V Cenni[1], K Scotlandi[3], MT Marino[3], L Merlini[2], S Squarzoni[1] and G Lattanzi*[,1]

Lamin A is a nuclear lamina constituent expressed in differentiated cells. Mutations in the *LMNA* gene cause several diseases, including muscular dystrophy and cardiomyopathy. Among the nuclear envelope partners of lamin A are Sad1 and UNC84 domain-containing protein 1 (SUN1) and Sad1 and UNC84 domain-containing protein 2 (SUN2), which mediate nucleo-cytoskeleton interactions critical to the anchorage of nuclei. In this study, we show that differentiating human myoblasts accumulate farnesylated prelamin A, which elicits upregulation and recruitment of SUN1 to the nuclear envelope and favors SUN2 enrichment at the nuclear poles. Indeed, impairment of prelamin A farnesylation alters SUN1 recruitment and SUN2 localization. Moreover, nuclear positioning in myotubes is severely affected in the absence of farnesylated prelamin A. Importantly, reduced prelamin A and SUN1 levels are observed in Emery–Dreifuss muscular dystrophy (EDMD) myoblasts, concomitant with altered myonuclear positioning. These results demonstrate that the interplay between SUN1 and farnesylated prelamin A contributes to nuclear positioning in human myofibers and may be implicated in pathogenetic mechanisms.
Cell Death and Differentiation advance online publication, 11 February 2011; doi:10.1038/cdd.2010.183

Formation of multinucleated myotubes from cells committed towards myogenic differentiation is required to maintain muscle tissue homeostasis. Myotubes are formed through a two-step mechanism: primary myotubes are formed by fusion of lined-up myoblasts, whereas other committed cells are fused laterally to primary myotubes to form secondary myotubes. During this process, nuclei become regularly spaced and myonuclear domains are well defined in the cytoplasm. Noticeably, the mechanism regulating nuclear positioning in myotubes involves critical transcription factors, such as NFATc and FHL1,[1] cytoskeleton constituents, including desmin[2] and tubulins, and an increasing number of nuclear envelope proteins, such as nesprins, SUN1, and SUN2.[3]

SUN proteins are integral proteins of the nuclear envelope known to anchor nesprins to the nucleoskeleton.[4] SUN1 has been shown to form dimers and heterodimers with SUN2 and to reside in the inner nuclear membrane of mammalian cells, with its C-terminal moiety in the perinuclear space.[5] SUN proteins have been reported to anchor centrosomes to centromere clusters.[6] Recent reports show that they have a role in skeletal muscle,[3] and SUN2 has been involved in the proper positioning of nuclei at the human neuromuscular junctions (NMJ) and in mouse myofibers, a function affected by lamin A pathogenetic mutations.[7] These data have provided increasing evidence of a functional link between the cytoskeleton and the nucleus potentially implicated in myogenic differentiation. However, partners regulating the dynamic behavior of SUNs and nesprins in the myoblast nuclear envelope have been elusive.

Recently, defective nuclear anchorage has been linked to mutations or absence of lamin A/C.[7,8] Lamins A and C are major constituents of the nuclear lamina produced by alternative splicing from the *LMNA* gene. They have been implicated in various functions, including nuclear stability, transcriptional control, cell cycle regulation, nucleo-cytoplasmic interplay, cellular signaling, and heterochromatin dynamics.[8–11] Although lamin A is ubiquitously expressed in differentiated tissues, a key role of lamin A in skeletal muscle is demonstrated by several published data showing its involvement in cell cycle exit,[12] cellular signaling,[13] induction of muscle-specific genes,[14] and nuclear positioning at the NMJ.[7] Mutations in the *LMNA* gene cause skeletal and cardiac muscle disorders in Emery–Dreifuss muscular dystrophy (EDMD), limb-girdle muscular dystrophy type 1B, or dilated cardiomyopathy with conduction defect.[9] Moreover, muscle atrophy or misfunctioning has been reported in progeroid disorders linked to lamin A mutations, such as Hutchinson–Gilford progeria,[15] mandibuloacral dysplasia,[16,17] and atypical Werner syndrome. These and other diseases caused by mutations in lamins or lamin-binding proteins are referred to as laminopathies or nuclear envelopathies.

In the context of lamin A-related disorders, prelamin A, the precursor protein of lamin A, has emerged as a key pathogenic factor.[10] Newly translated prelamin A undergoes a

[1]Institute for Molecular Genetics, IGM-CNR, Unit of Bologna, Bologna, Italy; [2]Laboratory of Musculoskeletal Cell Biology, Istituto Ortopedico Rizzoli, Bologna, Italy and [3]Laboratory of Oncological Research, Istituto Ortopedico Rizzoli, Bologna, Italy
*Corresponding author: G Lattanzi, Institute for Molecular Genetics, IGM-CNR, Unit of Bologna c/o IOR, Via di Barbiano 1/10, I-40136 Bologna, Italy.
Tel: +39 051 6366394; Fax: +39 051 583593; E-mails: lattanzi@area.bo.cnr.it or giovanna.lattanzi@cnr.it
Keywords: muscle differentiation; nuclear positioning; muscular dystrophy; SUN1; prelamin A
Abbreviations: SUN1, Sad1 and UNC84 domain-containing protein 1; SUN2, Sad1 and UNC84 domain-containing protein 2; EDMD2, autosomal dominant Emery–Dreifuss muscular dystrophy; FITC, fluorescein isothiocyanate; RT-PCR, reverse transcriptase-polymerase chain reaction; TRITC, tetramethylrhodamine-6-isothiocyanate
Received 04.8.10; revised 12.11.10; accepted 06.12.10; Edited by G Cossu

rapid multi-step process, which triggers formation of three intermediate products: full-length farnesylated prelamin A, cleaved farnesylated prelamin A, and carboxymethylated farnesylated prelamin A. Proteolytic removal of the farnesylated C-terminus end is carried out by a specific endoprotease called ZMPSTE24 and yields mature lamin A.[18] A biological role of the lamin A precursor is also suggested by its modulation in normal cells, mostly during differentiation. Prelamin A has been shown to influence chromatin dynamics, emerin localization, nuclear import of the transcription factor SREBP1 in adipocytes, and early events of myoblast differentiation.[14,19–21]

In the reported study, we focused on prelamin A processing and SUN1 interplay in human muscle cells. We demonstrate that SUN1 is retained at the nuclear envelope of human muscle progenitors through farnesylated prelamin A-dependent mechanisms. In fact, impairment of prelamin A farnesylation abolishes SUN1 recruitment to myotube nuclei, leading to myonuclear clustering. Clustering of myonuclei also occurs in EDMD myotubes showing reduced prelamin A and SUN1 levels. On the other hand, increasing levels of farnesylated prelamin A and SUN1 in adult muscle are suggestive of a role of these proteins in muscle homeostasis.

Results and Discussion

SUN1 and farnesylated prelamin A are recruited to the nuclear envelope in differentiated muscle cells. Bright staining of SUN1 was observed in cycling myoblasts, but it was considerably reduced in resting myoblasts (Figure 1A, arrowheads) and started to increase in cells committed to differentiation (caveolin 3-positive mononucleated cells, Figure 1A). Conversely, labeling of SUN2 was not significantly changed in myoblast subpopulations at any stage (Figure 1A). Unexpectedly, SUN1 fluorescence intensity was enhanced in myotubes, whereas SUN2 staining increased in a lower percentage of myotube nuclei (Figure 1A). Moreover, farnesylated prelamin A was absent from cycling myoblasts, whereas it was detected in committed myoblasts and myotubes throughout the differentiation process (Figure 1A). In fact, 1188-2 anti-prelamin A antibody, which selectively binds farnesylated prelamin A[22] (Figure 1B), brightly stained the nuclear envelope and, less intensely, the nucleoplasm in all of the multinucleated cells (Figure 1A). Other anti-prelamin A antibodies, which were directed to non-farnesylated epitopes in the prelamin A C-terminus (Figure 1B), failed to stain prelamin A in human muscle cells, at any stage (Figure 1C and D). Although farnesylated prelamin A could not be detected in nuclear lysates, because of the low efficiency of 1188-2 antibody in western blot analysis, immunochemical analysis supported the finding that SUN1 levels were decreased in resting myoblasts, whereas they rose again in myotubes (Figure 1E and F, statistically significant increase of SUN1 in differentiated cell cultures, $P<0.05$). Intriguingly, a 200-kDa band, likely corresponding to a SUN1 dimer, was detected in myotubes, but not in cycling or resting cells (Figure 1E).[5] SUN2 expression was not significantly changed at any stage in nuclear lysates (Figure 1E and F). Thus, our results, in agreement with reported data,[14,23] showed modulation of SUN1 and prelamin A levels during myogenesis.

SUN2, farnesylated prelamin A, and SUN1 at the nuclear poles and in tissues. Next, we compared the localization of prelamin A and SUN proteins at the nuclear envelope of human muscle cells (Figure 2). Colocalization of farnesylated prelamin A and SUN1 was observed in committed myoblasts and myotubes (Figure 2A). Moreover, the mean fluorescence intensity of SUN2, prelamin A, and SUN1 was measured in cycling, resting cells, or differentiated myoblasts (300 nuclei per sample). The statistical analysis reported in Figure 2B shows parallel upregulation of proteins in myotubes. In-depth evaluation of protein localization in committed myoblasts and myotubes allowed us to show that, although the nuclear envelope protein emerin was evenly distributed in the nuclear membrane, SUN2 was concentrated at one or both the

Figure 1 SUN1, SUN2, and farnesylated prelamin A modulation in human muscle progenitors. (**A**) Cycling myoblasts (cycling), committed myoblasts (day 3, caveolin positive mononucleated cells), and myotubes (day 8, caveolin positive multinucleated cells) are shown. Cells negative for caveolin 3 staining in b–e, h–m, and p–s are resting myoblasts (indicated by arrowheads). Nuclei were stained with antibodies directed to SUN1 (a–e), SUN2 (g–m), or farnesylated prelamin A (o–s). Caveolin 3 was detected using tetramethylrhodamine-6-isothiocyanate (TRITC)-conjugated anti-mouse IgG (red), SUN1, SUN2, and prelamin A were detected using fluorescein isothiocyanate (FITC)-conjugated secondary antibodies (green). Nuclei shown in day 8 myoblasts were counterstained with DAPI (f, n and t). (**B**) Prelamin A forms detected by the three antibodies used in this study. Epitopes detected by anti-prelamin A antibodies are colored in light blue. Anti-prelamin A 1188-1 antibody detects full-length prelamin A (aminoacids 648–664, prelamin A-specific), Sc-6214 antibody binds full-length prelamin A (aminoacids 645–664), 1188-2 antibody detects farnesylated prelamin A (aminoacids 648–661 including farnesyl-cysteine 661 and devoid of the SIM sequence), but not full-length prelamin A.[22] The farnesyl group is depicted as 'F' within a green circle. The prelamin A-specific sequence starts at aminoacid 648 (yellow bar). (**C**) Cycling myoblasts (a–c), day 3 myoblasts (d–f), and day 8 myoblasts (g–i) were labeled using three different anti-prelamin A antibodies (green). The code of each antibody is reported on the left. Cytoplasms were stained with anti-desmin antibody, as a muscle-specific marker (red staining). (**D**) The percentage of nuclei showing prelamin A staining, detected by antibodies 1188-1, Sc-6214 or 1188-2 is reported in the graph as means ± S.D. of three different counts (100 nuclei per count). Examined samples are: cycling myoblasts (cycling), resting myoblasts (resting), myotubes, and committed cells (myotubes). Asterisks indicate statistically significant differences at the Student's *t*-test ($P<0.05$), with respect to resting myoblast values. Samples were obtained from three different donors. (**E**) Western blot analysis of SUN1, SUN2, lamin A/C, and myogenin was performed in nuclear lysates from cycling myoblasts (cycling), day 3 myoblasts (day 3), or day 8 myoblasts (day 8). Myogenin was used as a differentiation marker. Ponceau staining of a representative band shows equal protein loading. Western blot analysis showing different stability of the SUN1 200 kDa band (asterisk) under reducing or nonreducing conditions is shown in the lower panel. 2-Me, 2-mercaptoethanol; 70°C, samples heated at 70°C in the presence of 2-mercaptoethanol. Equal number of nuclei was loaded per each sample. Myogenin is used as a differentiation marker also showing equal protein loading. Molecular weight markers are reported in kDa. Experiments were repeated three times under the same conditions. (**F**) Densitometric analysis of SUN1 (100 kDa) and SUN2 immunoblotted bands was performed in triplicate experiments, and the mean values ± S.D. are reported. Statistically significant differences ($P<0.05$), with respect to values determined in day 3 myoblasts are indicated by asterisks in the bars. Cycling, cycling myoblasts; day3, day 3 post-confluence; day8, day 8 post-confluence. Bars in (**A**) and (**C**), 10 μm

nuclear poles in about 60% of nuclei (Figure 2C–G). Farnesylated prelamin A was localized along the nuclear rim, but it was enriched at the nuclear poles in more than 60% of myotube nuclei (Figure 2C–G). SUN1 was enriched on one side of the nuclear envelope, possibly corresponding to the site of attachment of the microtubule-organizing center, in 35% of myotube nuclei (Figure 2C–G). However, double immunofluorescence staining of FLAG-tagged farnesylated prelamin A and SUN2 showed colocalization at the nuclear poles (Figure 2D). Both statistical analysis (Figure 2E) and examination of fluorescence intensity profile of the nuclear envelope (Figure 2G) confirmed polarization of SUN2, prelamin A, and SUN1 in committed myoblasts and myotubes. The nuclear poles are the extremities of the major axis of the cell nucleus. They anchor cytoskeletal proteins implicated in nuclear movement. Thus, the data reported here hint at a key role of SUNs and farnesylated prelamin A in myonuclear positioning.

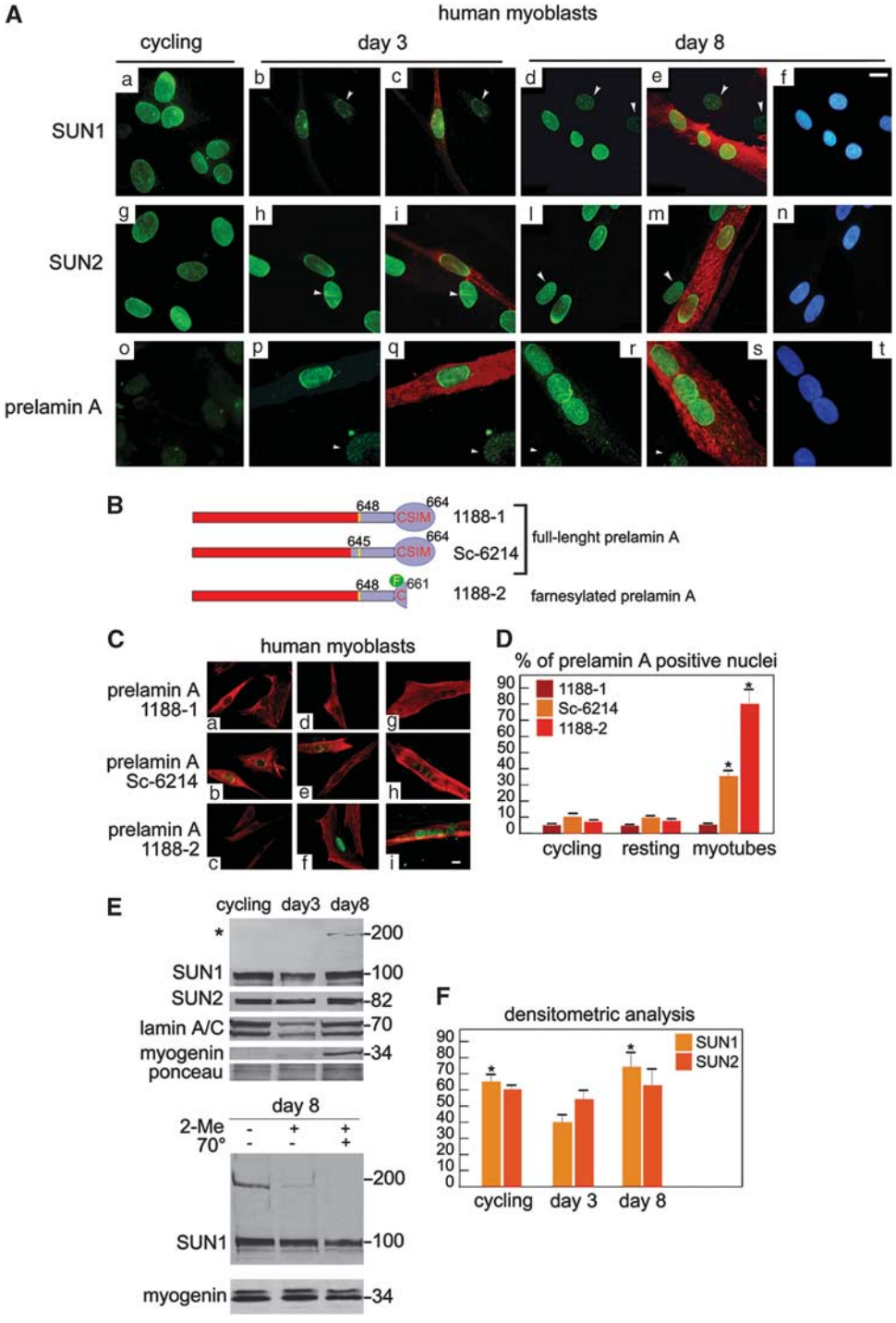

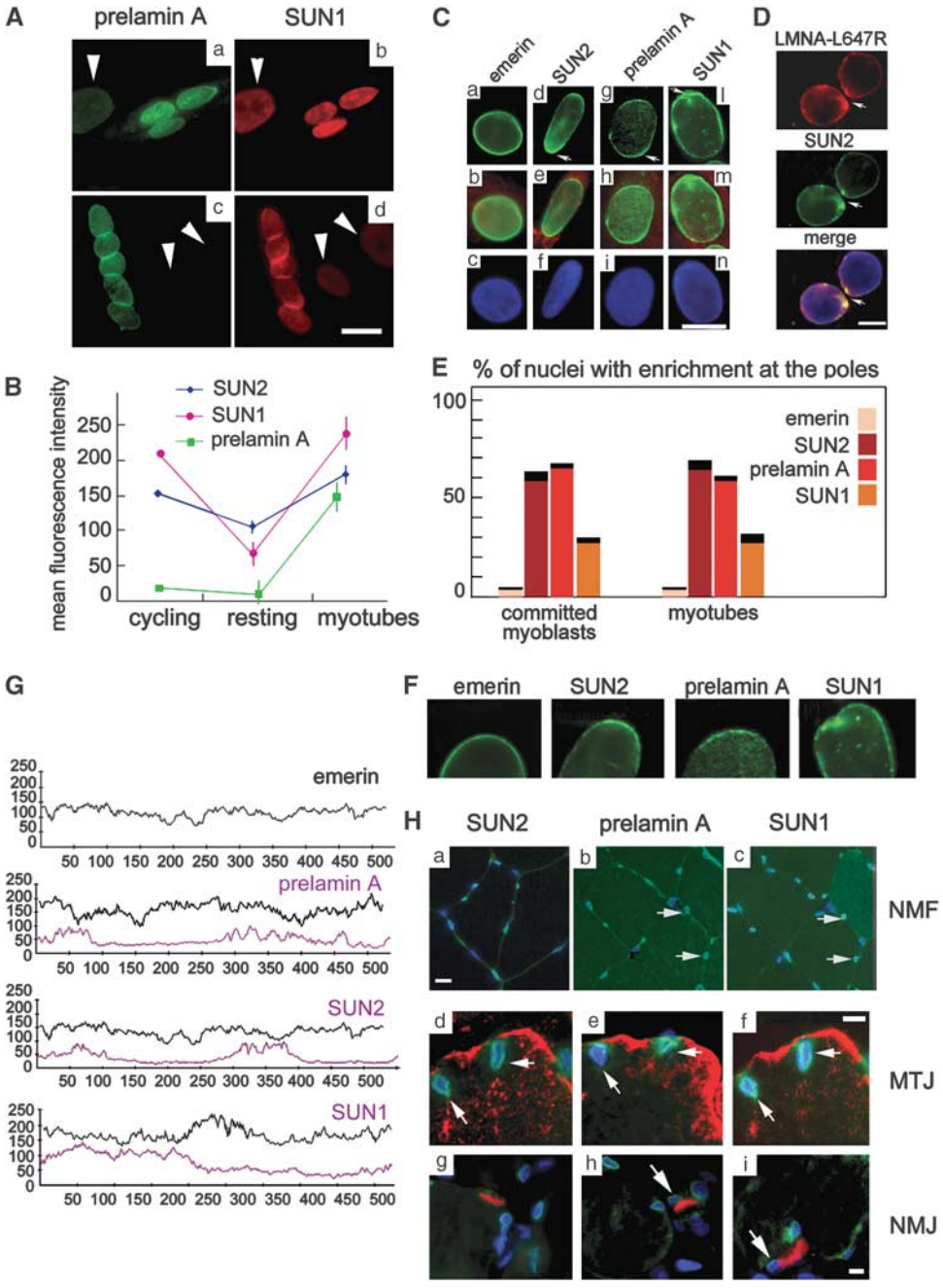

Figure 2 Localization of SUN1, SUN2, and prelamin A in human muscle cells. (**A**) Colocalization of farnesylated prelamin A (prelamin A, green) and SUN1 (SUN1, red) in human myotubes (day 8 post-confluence). Prelamin A staining is not observed in resting cells (arrowheads), whereas SUN1 levels are reduced. Bar, 10 μm. (**B**) Mean fluorescence intensity of SUN2, SUN1, and prelamin A in nuclei of cycling myoblasts (cycling), resting myoblasts (resting), and myotubes (myotubes) measured by the NIS software analysis system. 300 nuclei per sample were counted. (**C**) Emerin (a and b), SUN2 (d and e), farnesylated prelamin A (g and h), and SUN1 (l and m) were labeled using specific antibodies and detected using fluorescein isothiocyanate (FITC)-conjugated secondary antibodies (green). Caveolin 3 (red) was used as a differentiation marker (b, e, h and m). Counterstaining of DNA with DAPI is shown in c, f, i and n. Arrows indicate protein enrichment at the nuclear poles. (**D**) Differentiated myoblasts transfected with FLAG-tagged LA-L647R prelamin A were labeled using anti-FLAG (red) and anti-SUN2 (green) antibodies. Colocalization of proteins (arrows) and DAPI counterstaining are shown in the merged image (merge). (**E**) The percentage of nuclei with enrichment of staining at the nuclear pole(s) is reported in the graph as mean values ± S.D. of three different counts. One hundred of nuclei per each experiment were counted. Examined samples were committed myoblasts or myotubes, as reported below the bars. (**F**) Higher magnification of nuclear poles labeled by anti-emerin, SUN2, prelamin A, or SUN1 antibodies shows polarization of proteins. (**G**) Fluorescence intensity profile of the nuclear rim from cells co-stained using anti-emerin and anti-SUN2, prelamin A, or SUN1 antibodies. Analysis was performed using NIS elements 2.2, on 50 labeled nuclei per sample. Emerin profile was uniform (upper left panel and black profile in the other panels) and it was used as a control of nuclear shape. (**H**) SUN2, prelamin A, and SUN1 staining in cryosections from human paravertebral muscles (100 nuclei in each sample from three different biopsies). Non-synaptic muscle fibers (NMF) are shown in a, b and c. MTJ are shown in d–f (sarcolemma was labeled using anti-β 1D integrin antibody). NMJ are shown in g–i: acetylcoline receptors were stained using Texas red-conjugated α-bungarotoxin (red). Corresponding nuclei in serial cryosections are indicated by arrows. All the bars, 10 μm

Localization of SUN proteins and prelamin A was also investigated in mature muscle. We observed SUN1, SUN2, and prelamin A labeling at the nuclear envelope of myofibers (Figure 2H). The nuclear envelope constituents were also detected at the myotendinous junctions (MTJ), identified by integrin β 1D labeling (Figure 2H), and at the NMJ, labeled by α-bungarotoxin staining of acetylcoline receptors (Figure 2H). Colocalization of SUN2, farnesylated prelamin A, and SUN1 was observed in the same nuclei in serial muscle sections (Figure 2H).

Overexpression of farnesylated prelamin A enhances SUN1 levels. As it had been reported that recruitment of SUN1 to the nuclear envelope is mediated by prelamin A,[24,25] and we had shown that prelamin A levels are increased in differentiating mouse muscle,[14] we investigated a mechanistic role of prelamin A in SUN1 recruitment in human myoblasts.

To evaluate prelamin A's effects on SUN1 recruitment, we transfected HEK293 cells with prelamin A constructs. Wild-type prelamin A (LA-WT), which is processed to mature lamin A, LA-C661M prelamin A, which cannot be farnesylated, and LA-L647R prelamin A, which is farnesylated, but cannot undergo endoproteolysis (Figure 3a), were overexpressed in nuclei. In HEK293 cells, overexpression of farnesylated prelamin A caused a striking increase of SUN1 and SUN2 staining at the nuclear envelope (Figure 3b). It is noteworthy that basal levels of SUN1 and SUN2 fluorescence intensity were very low in HEK293 cells (Figure 3b). Western blot analysis confirmed that overexpression of prelamin A causes upregulation of SUN1 (Figure 3c). SUN2 levels were not affected, as determined by western blot analysis (Figure 3c), suggesting an increased accessibility of native SUN2 to IF antibody labeling in transfected HEK293 cells. Moreover, we found that farnesylated prelamin A, but not other prelamin A constructs, co-immunoprecipitated SUN1 *in vivo* (Figure 3c). However, a double-prelamin A mutant (LA-L647R/R527P), carrying the pathogenetic R527P *LMNA* mutation that hinders SUN1 binding,[26] failed to bind prelamin A (Figure 3c), suggesting that some other interaction in the lamin A/C domain is required to stabilize prelamin A binding. Conversely, SUN2 and emerin bound any prelamin A form with the same affinity (Figure 3c). To evaluate possible transcriptional regulation of SUN1 by farnesylated prelamin A, we analyzed SUN1 transcripts. The real-time reverse transcriptase-PCR (RT-PCR) analysis showed a threefold upregulation of SUN1 expression in cells overexpressing farnesylated prelamin A, but a downregulation of transcripts in the presence of non-farnesylated prelamin A (Figure 3d). We further hypothesized that prelamin A binding might stabilize SUN1 at the nuclear envelope in transfected HEK293 cells. Treatment of untransfected cells with the proteasome inhibitor MG132 or the lysosome inhibitor chloroquine (CQ) increased SUN1 levels, indicating that degradation of SUN1 does occur in HEK293 cells, whereas prelamin A accumulation mimics inhibition of the degradation pathways (Figure 3e). Consistent with the possibility that prelamin A anchors and stabilizes SUN1 at the nuclear envelope, we found that overexpression of the double-prelamin A mutant that is unable to bind SUN1 (LA L647R/R527P, Figure 3c),[26] while triggering SUN1 mRNA expression (Figure 3d), failed to increase SUN1 staining in nuclei (Figure 3c and f). Thus, both increased mRNA levels and protein anchorage contribute to SUN1 recruitment to the nuclear envelope.

It has been recently shown that SUN1 recruitment at the nuclear envelope of progeria fibroblasts accumulates prelamin A,[26] suggesting that recruitment of SUN1 by prelamin A occurs in diverse cell types. This hypothesis was supported by data obtained in human myoblasts. Although overexpression of prelamin A in cycling myoblasts did not significantly affect SUN1 or SUN2 staining in the majority of nuclei (Figure 1, Supplementary material), overexpression of prelamin A mutants in resting myoblasts influenced SUN1 staining at the nuclear envelope (Figure 3g). SUN2 fluorescence intensity was not significantly affected by prelamin A in transfected myoblasts (Figure 3g). SUN1 labeling was increased in cells transfected with uncleavable prelamin A (LA-L647R), whereas a variable effect was obtained using LA-WT and LA-C661M (Figure 3g). We could not completely rule out that SUN1-containing complexes, more tightly associated with insoluble structures, may include non-farnesylated prelamin A, because colocalization of non-farnesylated prelamin A and SUN1 was observed at the nuclear rim and in nuclear aggregates (Figure 3g). However, the whole evaluation of the above reported data allowed us to conclude that farnesylated prelamin A is the only form of the lamin A precursor recovered in normal differentiating human myoblasts and mature muscle, and to suggest that prelamin A influences SUN1 anchorage at the nuclear envelope of differentiating human muscle cells.

Mislocalization of prelamin A and SUN2 in mevinolin-treated myotubes. To start addressing the relevance of prelamin A farnesylation and SUN1 modulation in human muscle, we wondered whether changes in the post-translational modification harbored by prelamin A would have affected SUN1 expression and/or myoblast differentiation. Hence, we treated differentiating human myoblasts with mevinolin, an HMG-CoA reductase inhibitor known to impair farnesylation of prelamin A, thus eliciting accumulation of the non-farnesylated lamin A precursor.

In mevinolin-treated samples, we evaluated prelamin A localization, SUN1 and SUN2 staining, and myonuclear distribution.

As expected, 1188-2 antibody stained untreated myotube cultures, but failed to label mevinolin-treated cells (Figure 4A, panels a and b). Consistently, antibodies directed to full-length prelamin A brightly stained the nuclear envelope in mevinolin-treated cells, whereas they did not stain untreated samples (Figure 4A, panels c–f show antibody 1188-1 staining). Non-farnesylated prelamin A was not enriched at the nuclear poles, contrary to what was observed for the farnesylated form, but it was evenly distributed along the nuclear rim in most of the examined nuclei (Figure 4A, panels d and f). A minor percentage of nuclei showed mislocalization of non-farnesylated prelamin A and formation of enlarged aggregates (Figure 4A, panel f). The intensity of SUN2 fluorescence staining was not or was slightly affected by mevinolin treatment (Figure 4A, panels g–l). However, enrichment of SUN2 at the nuclear poles was completely lost in treated cells

(Figures 4A, panels h, l and statistics in 4B). These observations suggested that a specific localization of prelamin A and SUN2 in myotubes is maintained through an intermediate binding partner recruited by farnesylated prelamin A, whereas other prelamin A forms and/or mature lamin A anchor SUN2 all over the nuclear envelope.

SUN1 recruitment is reduced in mevinolin-treated myotubes. Treatment of cycling myoblasts with mevinolin did not affect SUN1 levels (Figure 2, see Supplementary material). However, the increase in SUN1 staining observed in control myotubes was not detectable in 60–70% of myotubes subjected to mevinolin treatment (Figures 4A, panels n, p and statistics in Figure 4C). This result demonstrated that accumulation of farnesylated prelamin A, but not its unprocessed form, causes upregulation and recruitment of SUN1 to the nuclear envelope in human myotubes. Indeed, SUN1 protein levels were reduced in cells subjected to mevinolin treatment, as determined by western blot analysis (Figure 4C). Overexpression of FLAG-prelamin A in human myotubes supported these results (Figure 1, see Supplementary material). In cells overexpressing wild-type

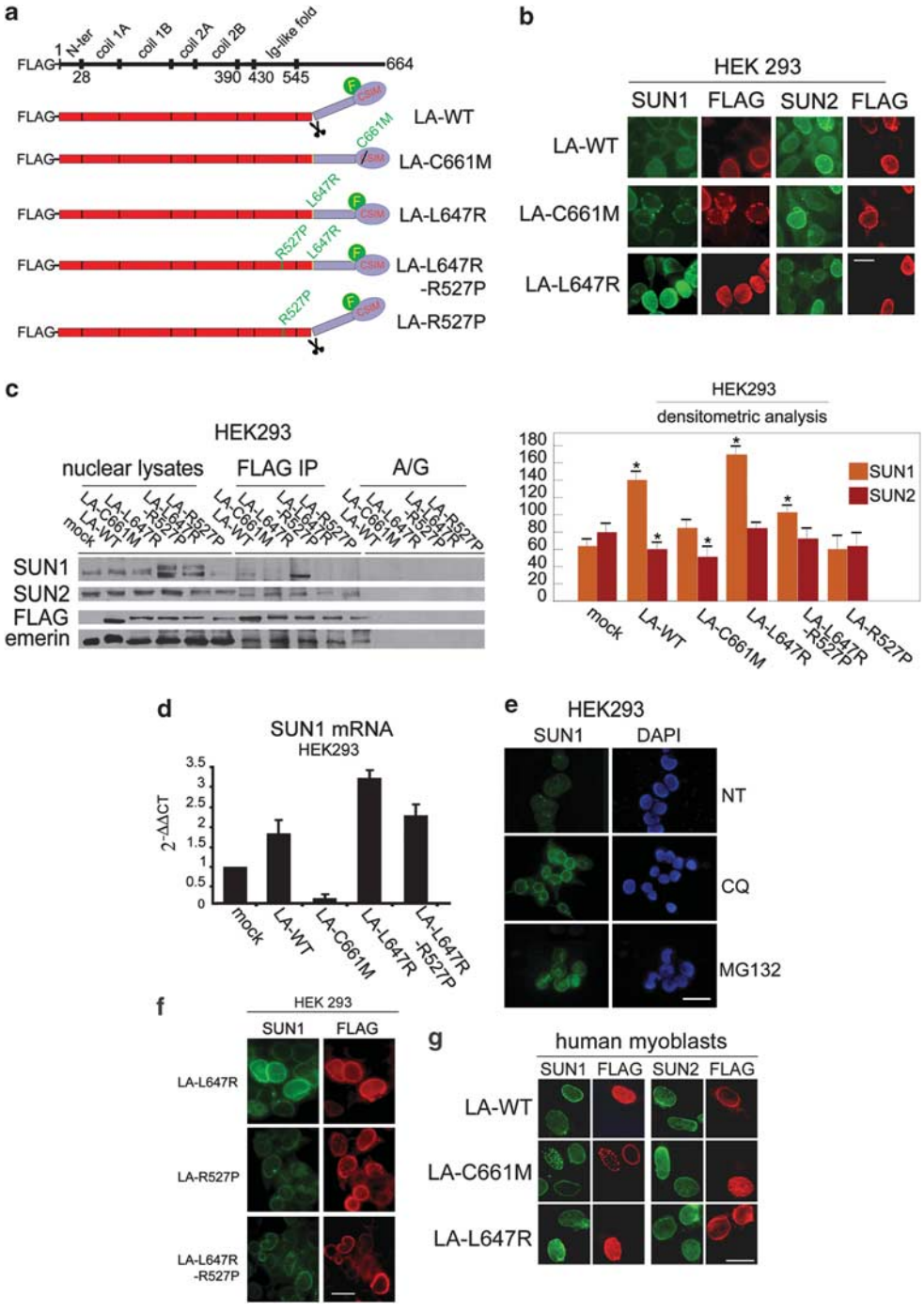

prelamin A or LA-L647R prelamin A, SUN1 levels were not substantially affected (Figure 1, see Supplementary material). We interpreted these results by considering that accumulation of SUN1 in the nuclear envelope (that occurs in untransfected myotubes) cannot be further enhanced by overexpression of farnesylated prelamin A. Conversely, in agreement with the effect observed in mevinolin-treated cells, overexpression of LA-C661M, which elicits accumulation of non-farnesylated prelamin A, lowered SUN1 levels in 30% of myotube nuclei (Figure 1, see Supplementary material). Since accumulation of non-farnesylated prelamin A in cycling myoblasts did not influence SUN1 levels, and endogenous prelamin A was not detected at that stage, we suggest that SUN1 expression in cycling muscle cells may be regulated by other factors. Moreover, SUN2 protein levels, which were not affected by mevinolin treatment (Figure 4C), appear to be independent of prelamin A.

Clustering of nuclei in myotubes accumulating non-farnesylated prelamin A. Myotubes treated with mevinolin showed mislocalization of nuclei into enlarged clusters at the extremities of multinucleated cells (Figures 4A and statistics in B, $P<0.05$ in treated *versus* untreated myotubes). Further, we found unordered arrangement of myonuclei within each cluster, along with high variability of myonuclear size and morphology (Figure 4A and statistics in B). These results indicated that farnesylated prelamin A is involved in myonuclear anchorage or incorporation within myotubes. Clustering of nuclei mostly occurred in myotubes showing well-organized sarcomeres and more than 12 nuclei (Figure 4A, panels b, f, l and p), suggesting that farnesylated prelamin A could have a major role in the formation of secondary myotubes. Along this line, recent reports show that SUN1 and SUN2 have a critical role in nuclear positioning in mouse muscle.[7] Moreover, altered organization of nuclei at the NMJ, associated with SUN2 mislocalization, has been demonstrated in muscles from laminopathic mouse models.[13] Regarding the role of prelamin A and SUNs in nuclear positioning, we propose the following mechanism. Farnesylated prelamin A accumulation triggers upregulation of SUN1 and favors localization of SUN2 at the nuclear poles. Both SUN1 and SUN2, known to interact with centrosomal constituents,[6,27] drive nuclear movement through cytoskeleton binding. In this context, a role of the prelamin A and SUN1 binding partner emerin, implicated in centrosome positioning[28] and undergoing modulation and cytoskeleton binding during myogenesis,[29,30] appears likely. However, an interplay between SUNs, prelamin A, and centrosomal proteins in human myoblasts deserves further investigation.

Physiological relevance of SUN1–prelamin A interplay. Persistence of SUN1 and prelamin A in mature muscle hinted at the existence of a molecular complex involved not only in myogenesis, but also in muscle homeostasis. To evaluate the physiological relevance of SUN1–prelamin A interplay, we examined protein distribution in human myofibers at different ages. Prelamin A and SUN1 underwent parallel modulation, with myofibers from younger individuals (4 months) showing faint or absent labeling of both proteins at the nuclear rim (Figure 5A). SUN1 and prelamin A staining increased in adult and aged muscle. Bright staining of both nuclear constituents was observed starting at age 20 up to age 82 in all muscle and connective tissue nuclei (Figure 5A). The modulation of prelamin A and SUN1 levels here, shown during muscle development and ageing (Figures 5A and B), is consistent with the possibility that both proteins might regulate nucleo-cytoskeleton relationships in adult to aged muscle. Importantly, it has been shown that SUN proteins are dispensable for muscle development in the embryo, while they have a key role in muscle homeostasis.[7] Moreover, it has been reported that myonuclear domains are differently organized in young, adult, or aged muscle, suggesting age-related modulation of proteins, such as SUN1, regulating nuclear positioning, and cytoskeleton interplay.

Low farnesylated prelamin A and SUN1 levels in EDMD myoblasts associated with clustering of myonuclei. *LMNA* mutations causing muscle laminopathies may interfere with prelamin A–SUN1 interaction.[26] Moreover, altered myonuclear positioning and chromatin defects have been

Figure 3 Potential mechanisms of SUN1 regulation by prelamin A. (**a**) Prelamin A sequences expressed in this study. Cells were transfected with cDNAs encoding for LA-WT (processable prelamin A), LA-C661M (non-farnesylable prelamin A) or LA-L647R (uncleavable farnesylated prelamin A) LA-L647R/R527 prelamin A double mutant, and LA-R527H processable prelamin A. Protein domains are reported in figure row. Mutations are reported in green. (**b**) SUN1 and SUN2 expression in HEK 293 cells transfected with prelamin A forms. The percentage of transfected cells ranged 80–90%. SUN1 and SUN2 were labeled using specific antibodies and revealed by fluorescein isothiocyanate (FITC)-conjugated secondary antibody (green). Overexpressed proteins were detected using a Cy3-conjugated anti-FLAG antibody (red). (**c**) Left panel: western blot analysis of SUN1 and SUN2 in transfected HEK293 cells was performed using nuclear lysates (nuclear lysates). Mock, mock-transfected cells. Co-immunoprecipitation of FLAG-tagged prelamin A and SUNs was performed using an anti-FLAG antibody (FLAG-IP) in nuclear lysates. Proteins were detected using anti-SUN1, SUN2, FLAG or emerin antibody. SUN1 co-immunoprecipitated with LA-L647R prelamin A only. A/G, control precipitations performed with antibody free buffer. Right panel: densitometric analysis of SUN1 and SUN2 immunoblotted bands obtained from HEK293 nuclear lysates analyzed in triplicate western blots. Mean values ± S.D. are reported. Statistically significant differences with respect to mock transfected cells values were determined by Student's *t*-test ($P<0.05$). (**d**) Real-time RT-PCR of SUN1 transcripts in HEK293 cells mock-transfected (mock) or transfected with LA-WT, LA-C661M, LA-L647R or LA-L647R/R527P for 24 h. LA-C661M elicits SUN1 downregulation, whereas LA-L647R causes a threefold upregulation of SUN1. (**e**) Accumulation of SUN1 at the nuclear envelope in HEK293 cells treated with the lysosome inhibitor CQ or the proteasome inhibitor MG132 (MG132). SUN1 was stained with specific antibody and revealed by FITC-conjugated secondary antibody (green). Nuclei were counterstained with DAPI. (**f**) Overexpression of mutant prelamin A, which cannot bind SUN1 (LA-R527P or LA-L647R/R527P), fails to elicit recruitment of SUN1 to the nuclear envelope. LA-L647R farnesylated prelamin A was overexpressed as a positive control. Overexpressed proteins were revealed by Cy3-conjugated anti-FLAG antibody (red), SUN1 was labeled with specific antibody (green). (**g**) Human myoblasts (resting cells, day 3 post-confluence) were transfected with LA-WT, LA-C661M or LA-L647R cDNAs and fixed 48 h after transfection. SUN1 and SUN2 were labeled using specific antibodies and revealed by FITC-conjugated secondary antibody (green). Overexpressed proteins were detected using Cy3-conjugated anti-FLAG antibody (red). Bars in (**b**), (**e**), (**f**), and (**g**), 10 μm

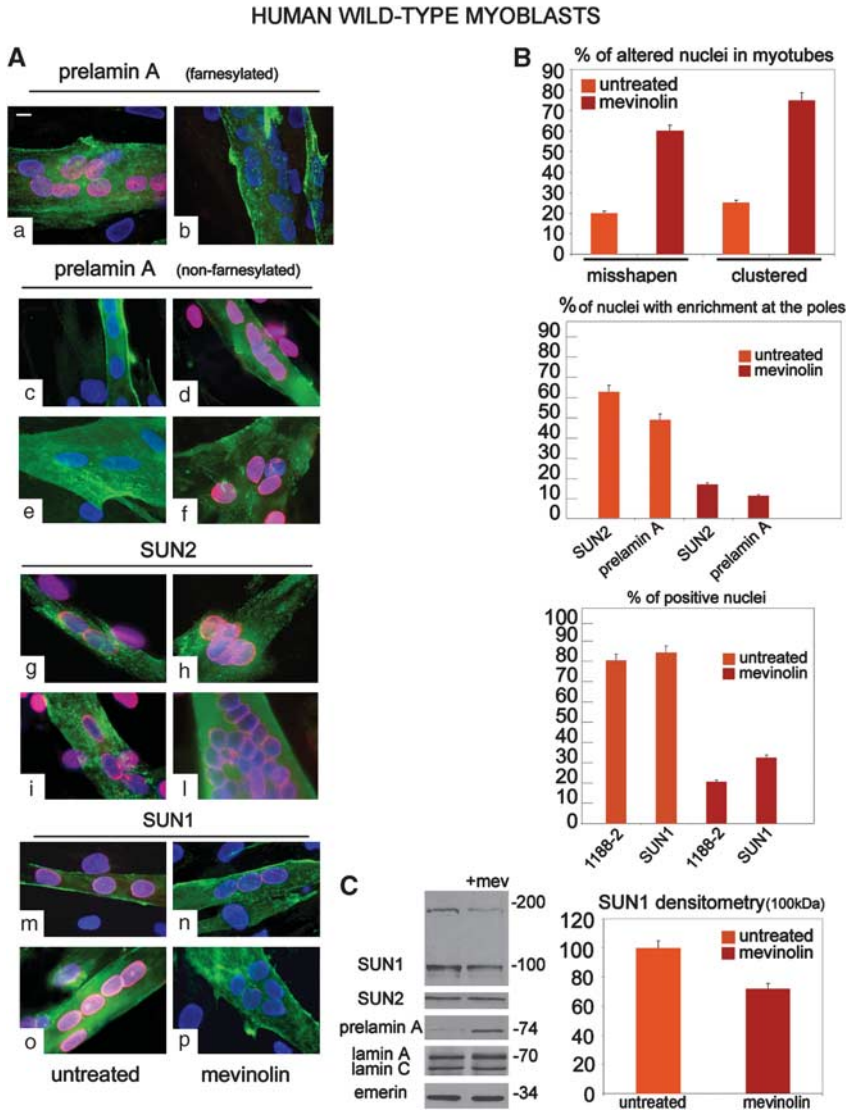

Figure 4 Reduced levels of farnesylated prelamin A affect SUN1 expression and nuclear positioning in myotubes. (**A**) Differentiating myoblasts (day 6 post-confluence) were left untreated (untreated) or treated with mevinolin for 48 h (mevinolin). Cell cultures were fixed at day 8 post-confluence. Highly differentiated myotubes (more than 12 nuclei) are shown in a, b, e, f, i, l, o and p. Myotubes with less than six nuclei are shown in c, d, g, h, m and n. Farnesylated prelamin A was detected using 1188-2 antibody (a, b, red). Full-length prelamin A (non-farnesylated prelamin A) was detected using 1188-1 antibody (c–f, red). SUN2 was detected using anti-SUN2 antibody (g–l, red). SUN1 was detected using anti-SUN1 antibody (m–p, red). Caveolin 3 (green) was stained as a marker of myogenic differentiation. Bar, 10 μm. Clustering of myotube nuclei (more than three agglomerated nuclei in unordered distribution on one side of the myotube, with myotube areas devoid of nuclei) is observed in mevinolin-treated cells (right lane). Misshapen nuclei (nuclei with blebs, invaginations, or enlarged nuclei) are also observed (d, f, h). (**B**) Statistical analysis (mean values ± S.D. of counts performed in three different samples). Counting was performed in 100 myotube nuclei per each sample. Misshapen nuclei (misshapen) or nuclei belonging to a cluster (clustered) were counted in myotubes left untreated or treated with mevinolin (upper panel). Nuclei showing nuclear pole enrichment of SUN2 (detected using anti-SUN2 antibody) or prelamin A (detected using anti-prelamin A 1188-2 antibody in untreated cells and anti-prelamin A 1188-1 antibody in mevinolin-treated cells) were counted (middle panel). SUN1 or farnesylated prelamin A fluorescence intensity, labeled using anti-SUN1 or anti-prelamin A 1188-2 antibody, respectively, was determined using the NIS software and registered for 100 nuclei (lower panel). All the differences between untreated and mevinolin-treated samples were statistically significant ($P<0.05$). (**C**) Western blotting analysis of SUN1, SUN2, prelamin A, and lamin A/C in untreated or mevinolin-treated (+ mev) myotube cultures. Prelamin A was detected using anti-prelamin A 1188-1 antibody directed to the full-length protein. Emerin is used as a loading control. Molecular weight markers are reported in kDa. Densitometric values are reported as percentage of values registered in untreated samples and represent means ± S.D. of three different experiments

reported in laminopathic muscle.[7,31] On the basis of these published data, and on the new findings here obtained in normal human muscle, we wondered if *LMNA* pathogenetic mutations might affect SUN1 expression or recruitment to the nuclear envelope. In autosomal dominant Emery–Dreifuss muscular dystrophy (EDMD2) myoblasts, we indeed observed lower levels of farnesylated prelamin A and SUN1 (Figures 5C and D), whereas non-farnesylated prelamin A was not detected. About 40% of myotube nuclei were negative for prelamin A and SUN1 labeling ($P<0.05$ in 100 counted nuclei from 3 different EDMD cultures *versus* controls). Importantly, highly differentiated myotubes showed nuclear clustering and misshapening (Figures 5C and D), reminiscent of what was observed in wild-type myotubes in the absence of farnesylated

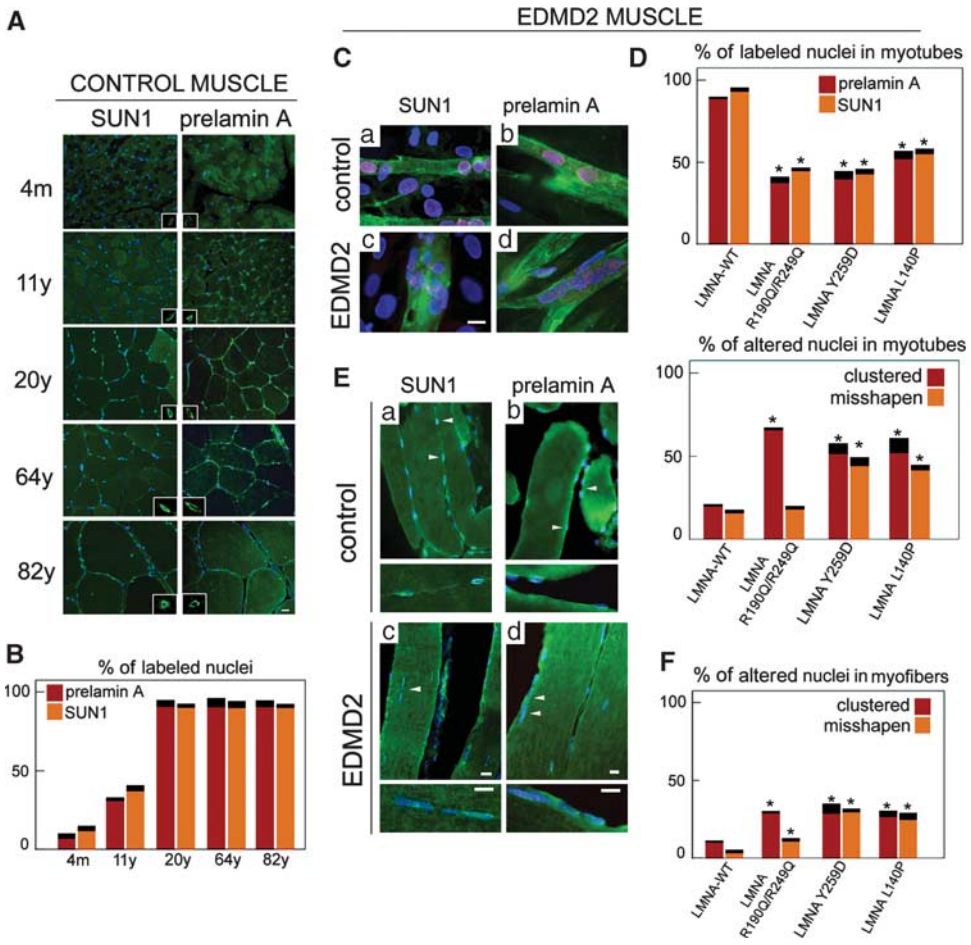

Figure 5 Physiological role of prelamin A/SUN1 interplay. (**A**) SUN1 and farnesylated prelamin A staining in muscle cryosections from tibialis anterior of individuals at different age (control muscle). Fluorescein isothiocyanate (FITC)-conjugated secondary antibodies were used to detect SUN1 and prelamin A (green). Nuclei were counterstained with DAPI. A representative nucleus at twofold magnification is shown in the inset for each picture. m, months; y, years. (**B**) The percentage of farnesylated prelamin A (prelamin A) or SUN1 (SUN1) positive nuclei is reported as mean value of three different countings performed in two different samples of the same age. m, months; y, years. (**C**) Myotubes from control (a and b) or EDMD2 (c and d) primary cultures were stained for farnesylated prelamin A (prelamin A) or SUN1 (SUN1) at day 8 post-confluence. Reduced protein levels and myonuclear clustering are observed in EDMD2 myotubes. Prelamin A and SUN1 were stained using specific antibodies and revealed by tetramethylrhodamine-6-isothiocyanate (TRITC)-conjugated secondary antibody (red). Caveolin 3 (green) was stained as a marker of myogenic differentiation. (**D**) Statistical analysis (mean values ± S.D. of three different countings) performed in control and EDMD2 myotubes. Mutations are reported below the bars. SUN1 (SUN1) or farnesylated prelamin A (prelamin A) fluorescence intensity, labeled using anti-SUN1 or anti-prelamin A 1188-2 antibody, respectively, was determined using the NIS software and registered for 100 nuclei (upper panel). Misshapen nuclei (misshapen) or nuclei belonging to a cluster (clustered) were counted and registered for 100 nuclei (lower panel). (**E**) Tibialis anterior muscle longitudinal sections from control (a,b and insets below each panel) or EDMD2 patients (c, d and insets below each panel) were stained for SUN1 (SUN1, a and c) or farnesylated prelamin A (prelamin A, b and d). Proteins were revealed by FITC-conjugated secondary antibody (green). Nuclei indicated by arrowheads are shown at threefold magnification in the insets. (**F**) Statistical analysis (mean values ± S.D. of three different countings) performed in control and EDMD2 myofibers. Misshapen nuclei (misshapen) or nuclei belonging to a cluster (clustered) were counted and registered. Fifty nuclei per sample were counted in longitudinal sections. Nuclei were counterstained with DAPI. Bars in (**A**), (**C**) and (**E**), 10 μm

prelamin A (Figure 4). In mature muscle, both SUN1 and prelamin A levels were slightly affected by *LMNA* mutations (Figure 5E). Nuclear clustering, however, was observed in longitudinal fibers (Figures 5E and F). We suggest that reduced prelamin A and SUN1 recruitment in EDMD2 primarily affects satellite cells activity and myotube formation. However, downstream effects including clustering of myonuclei may progressively accumulate in mature muscle.

Conclusion

The functional connection between the cytoskeleton and the nucleus involves proteins of the so-called LINC complex (after linker of cytoskeleton and nucleoskeleton), including SUNs and nesprins.[32] It is possible that SUN proteins not only regulate nuclear anchorage, but also coordinate positioning of chromatin domains with respect to that of the nucleus.[33] This intriguing function appears to be particularly relevant in differentiating myoblast nuclei, which undergo dramatic changes in their structure, location, and higher order chromatin arrangement.

Here we show that SUN1 expression is modulated during differentiation of human muscle progenitors in a farnesylated prelamin A-dependent way. Our data further hint at the existence of a molecular complex including SUN1 and prelamin A, which could be involved in adult muscle

homeostasis. The interplay between prelamin A and SUN proteins is implicated in myonuclear positioning in healthy human muscle. Hence, myonuclear positioning is affected by the low levels of farnesylated prelamin A and SUN1 found in EDMD2 myoblasts. Thus, we suggest that prelamin A levels and post-translational modifications are crucial to protein functionality in myogenic progenitors.

The perspective of our study will be to identify modulators of prelamin A levels, as well as other binding partners of farnesylated prelamin A and/or SUNs, relevant to the described effects in human muscle. For instance, FHL1, nesprin 1 and 2 represent good candidates, because they are involved in myonuclear positioning[34,35] and myotube hypertrophy,[1] and are indeed mutated in EDMD.[36,37]

Our results suggest that muscle atrophy or misfunctioning found in progeria[15] and mandibuloacral dysplasia[16] could be related to impaired modulation of prelamin A processing and downstream effects on SUN1 recruitment.

On the other hand, it has been recently reported that accumulation of non-farnesylated prelamin A causes cardiomyopathy in mice.[38] This finding supports our observations in skeletal muscle and suggests that prelamin A–SUN1 interplay deserves investigation in cardiac myocytes. Finally, as hypothesized by diverse authors, it appears likely that mutations in SUN1 or SUN2 might be linked to laminopathies.

Materials and Methods

Cell culture and transfection. Human myoblast cultures were obtained from muscle biopsies by mechanical and enzymatic methods, as previously reported.[39] Biopsies were obtained from 10 consenting patients undergoing orthopedic surgery for traumas. Biopsies from three EDMD2 patients undergoing diagnosis were used to establish primary myoblast cultures or cryosectioned to analyze protein localization. All the local and EU ethical issues were respected. Mutations found in EDMD2 muscle were: *LMNA* R190Q/R249Q, *LMNA* Y259D, *LMNA* L140P.[39]

To obtain myotubes, confluent cell cultures were allowed to differentiate in culture medium (D-MEM plus 20% FCS plus antibiotics) for 8 days. Cells cultured for 3–4 days post-confluence were defined as resting cells if 4–8 myotubes per dish (P100 dishes) were counted. PCNA staining of these cultures was negative in 70% of nuclei.

HEK293 cells were transfected with FLAG-tagged plasmids containing wild-type prelamin A, LA-WT, which undergoes normal maturation, LA-C661M, which cannot be farnesylated, and LA-L647R, which is farnesylated but cannot undergo endoproteolysis[35] (Figure 3a). The LA-R527P and LA-L647R/R527P prelamin A constructs (Figure 3a), which carry the pathogenetic mutation R527P causing EDMD2,[26] were also transfected in HEK293 cells. Transfections were performed using calcium phosphate buffer, whereas human myoblasts and myotubes were transfected using an AMAXA electroporator (Amaxa, Loza Group, Basel, Switzerland), according to the manufacturer's instructions. After transfection, cells were incubated for 24–48 h.[14]

When indicated, the proteasome inhibitor MG132 (1 μM for 24 h) or the lysosomal activity inhibitor CQ-diphosphate (25 μM for 18 h) were added to transfected HEK293 cells to study SUN1 degradation.

Accumulation of non-farnesylated prelamin A was obtained using 10 μM mevinolin (Sigma, St. Louis, MO, USA) in growth medium for 48 h.[40]

Real-time PCR. Total RNA was extracted using the TRIzol extraction kit (Invitrogen, Milan, Italy). Real-time PCR was performed on the panel of HEK293 cells transfected with prelamin A constructs (LA-WT, LA-C661M, LA-L647R, LA-L647R/R527P, or the empty vector) for 24 h. In particular, 500 ng of total RNA was reverse-transcribed with high capacity cDNA archive kit (Applied Biosystems, Foster City, CA, USA). Gene-specific primers were designed using Beacon Designer software (Premier Biosoft International, Palo Alto CA, USA): SUN1 (accession no. NM_001130965.2), forward 5′-CAGAAGCACAAACAAATC-3′ and reverse 5′-CACCATCATCATCAAGAC-3′; glyceraldehyde-3-phosphate dehydrogenase (GAPDH) was amplified as endogenous control (forward 5′-GAAGGTGAA GGTCGGAGTC-3′ and reverse 5′-GAAGATGGTGATGGGATTTC-3′. Amplification was performed at the following cycling conditions: 95°C for 10 min, followed by 40 cycles at 95°C for 15 s and 55°C for 1 min. A SYBR Green PCR Master Mix (Applied Biosystems) was used with 5 ng of cDNA and with 300 nM primers. No template controls were run with every assay performed on ABI PRISM 7900 Sequence Detection System (Applied Biosystems). Data were normalized to GAPDH and expressed as relative amounts of SUN1 mRNA in transfected cell lines compared with the empty vector-transfected calibrator. All data are expressed as $2^{-\Delta\Delta CT}$. Data were obtained from triplicate experiments.

Immunofluorescence and immunohistochemistry. Cells were grown on glass coverslips, and immunofluorescence staining was performed in samples fixed in 100% methanol for 7 min. Unfixed cryosections were saturated for 45 min with 4% BSA before immunofluorescence reactions.[39]

Three different antibodies were used to detect prelamin A: antibody 1188-1 (Diatheva, Fano, Italy), which is directed against the last 15 amino acids of the full-length protein; antibody 1188-2 (Diatheva), which selectively binds farnesylated prelamin A devoid of the last three amino acids (Figure 3, see Supplementary material);[22] Sc-6214 anti-prelamin A antibody (Santa Cruz Inc., Santa Cruz, CA, USA), which is directed against the 20 C-terminal amino acids of the full-length lamin A precursor (Figure 1B). All prelamin A antibodies were used at 1 : 100 dilution, except 1188-2 antibody, which was used at 1 : 10 dilution. Rabbit polyclonal anti-SUN2 and -SUN1 antibodies[4,5] were from Atlas (Stockholm, Sweden) and were used at 1 : 800 and 1 : 300 dilution, respectively. Goat polyclonal anti-SUN1 was from Santa Cruz. Anti-caveolin 3 antibody (BD-Transduction, BD Biosciences, Franklin Lakes, NJ, USA) was diluted 1 : 30, anti-desmin (Novocastra, Newcastle, UK) was diluted 1 : 100, and anti-dystrophin (Novocastra) was incubated at 1 : 10 dilution. Texas red-conjugated α-bungarotoxin (Molecular Probes/Invitrogen, Carlsbad, CA, USA) was used to label NMJ. Anti-β1D integrin (Chemicon, Temecula, CA, USA) was used to recognize MTJ.

Immunofluorescence microscopy was performed using a Nikon E600 epifluorescence microscope and a Nikon oil-immersion objective (100 $\times$ magnification, 1.3 NA (numerical aperture)). Photographs were taken using a Nikon digital camera (DXm) and NIS-Element BR2.20 software (Nikon, Nikon Instruments, Calenzano, Firenze, Italy). All images were taken at similar exposures within an experiment for each antibody. Image quantification was performed using NIS-Element BR2.20 software.

Images were processed using Adobe Photoshop 7.0 software (Adobe Systems, Italia, Rome, Italy).

Nuclear fractioning. To obtain nuclear fractions, cells detached with trypsin were incubated in cold hypotonic buffer containing 10 mM Tris-HCl and protease inhibitors. Mechanical separation was then performed with a syringe and centrifugation of nuclei was performed at 1100 r.p.m. for 10 min. Nuclei were lysed in buffer containing 50 mM Tris-HCl, 1% SDS containing or not 5% 2-mercaptoethanol. Some samples were heated at 70°C to check the stability of SUN1 dimers, whereas other samples were obtained in the absence of 2-mercaptoethanol.[5] Lysates were subjected to SDS-PAGE and western blot analysis, as described below.

Immunoprecipitation and immunoblotting. Immunoprecipitation was performed in transfected HEK293 cells overexpressing prelamin A mutants, according to a procedure reported in previous studies.[21] Briefly, HEK293 cells were lysed in IP buffer containing 50 mM HEPES/HCl (pH 7.4), 100 mM NaCl, 1.5 mM $MgCl_2$, 1% NP-40, 1 mM dithiothreitol, 1 mM PMSF, and protease inhibitors. After sonication and clarification, 500 μg of each lysate were incubated with anti-FLAG antibody overnight at 4°C. Control immunoprecipitations were performed in the presence of nonspecific immunoglobulins. After addition of 30 μl of Protein A/G (Santa Cruz Biotechnology), lysates were incubated with continuous mixing at 4°C for 3 h. Immunoprecipitated protein complexes were subjected to western blot analysis.

Western blot analysis was performed on proteins separated by a 5–20% gradient SDS-PAGE. Nitrocellulose membranes were probed using the following antibodies: anti-FLAG (Sigma, 1 : 1000 dilution); rabbit polyclonal anti-SUN2 and SUN1 (Atlas, 1 : 200 and 1 : 100 dilution, respectively); anti-prelamin A (1188-1, Diatheva, 1 : 100 dilution); anti-emerin (Monosan, Uden, Netherlands, 1 : 100 dilution); anti-myogenin (Santa Cruz, 1 : 100 dilution). Immunoblotted bands were revealed by the Amersham ECL detection system (Glattbrugg, Switzerland). The intensity of bands was measured using a GS800 Densitometer (Bio-Rad Laboratories, Milan, Italy).

Statistical analysis. Statistical analysis was performed using Excel software (Microsoft, Microsoft Italia, Segrate, Milan, Italy). Statistically significant differences were determined using the Student's *t*-test.

Conflict of interest

The authors declare no conflict of interest.

Acknowledgements. We wish to thank William Blalock (Cell Signaling Laboratory, Department of Human Anatomical Sciences, University of Bologna) for revising the manuscript and for the helpful discussion, Clara Guerzoni for the evaluation of the expression study, and P Sabatelli, A Valmori, O Fiorani, S Grasso, and D Zini for the technical assistance. This work was supported by grants from A.I.Pro.Sa.B., Italy; EU-funded FP6 Euro-Laminopathies project; Italian MIUR PRIN 2008 to GL; ISS 'Rare Diseases Italy–USA program (Grant no. 526/D30); Telethon Grant no. GUP08006 to LM; and Fondazione Carisbo, Italy. We apologize to collegues and authors who have not been cited because of limits in the number of references.

1. Cowling BS, McGrath MJ, Nguyen MA, Cottle DL, Kee AJ, Brown S *et al.* Identification of FHL1 as a regulator of skeletal muscle mass: implications for human myopathy. *J Cell Biol* 2008; **183**: 1033–1048.
2. Milner DJ, Weitzer G, Tran D, Bradley A, Capetanaki Y. Disruption of muscle architecture and myocardial degeneration in mice lacking desmin. *J Cell Biol* 1996; **134**: 1255–1270.
3. Lei K, Zhang X, Ding X, Guo X, Chen M, Zhu B *et al.* SUN1 and SUN2 play critical but partially redundant roles in anchoring nuclei in skeletal muscle cells in mice. *Proc Natl Acad Sci USA* 2009; **106**: 10207–10212.
4. Padmakumar VC, Libotte T, Lu W, Zaim H, Abraham S, Noegel AA *et al.* The inner nuclear membrane protein Sun1 mediates the anchorage of Nesprin-2 to the nuclear envelope. *J Cell Sci* 2005; **118**(Part 15): 3419–3430.
5. Lu W, Gotzmann J, Sironi L, Jaeger VM, Schneider M, Luke Y *et al.* Sun1 forms immobile macromolecular assemblies at the nuclear envelope. *Biochim Biophys Acta* 2008; **1783**: 2415–2426.
6. Schulz I, Baumann O, Samereier M, Zoglmeier C, Graf R. Dictyostelium Sun1 is a dynamic membrane protein of both nuclear membranes and required for centrosomal association with clustered centromeres. *Eur J Cell Biol* 2009; **88**: 621–638.
7. Mejat A, Decostre V, Li J, Renou L, Kesari A, Hantai D *et al.* Lamin A/C-mediated neuromuscular junction defects in Emery-Dreifuss muscular dystrophy. *J Cell Biol* 2009; **184**: 31–44.
8. Mittelbronn M, Sullivan T, Stewart CL, Bornemann A. Myonuclear degeneration in LMNA null mice. *Brain Pathol* 2008; **18**: 338–343.
9. Marmiroli S, Bertacchini J, Beretti F, Cenni V, Guida M, De Pol A *et al.* A-type lamins and signaling: the PI 3-kinase/Akt pathway moves forward. *J Cell Physiol* 2009; **220**: 553–561.
10. Maraldi NM, Lattanzi G. Involvement of prelamin A in laminopathies. *Crit Rev Eukaryot Gene Expr* 2007; **17**: 317–334.
11. Hakelien AM, Delbarre E, Gaustad KG, Buendia B, Collas P. Expression of the myodystrophic R453W mutation of lamin A in C2C12 myoblasts causes promoter-specific and global epigenetic defects. *Exp Cell Res* 2008; **314**: 1869–1880.
12. Gotic I, Schmidt WM, Biadasiewicz K, Leschnik M, Spilka R, Braun J *et al.* Loss of LAP2alpha delays satellite cell differentiation and affects postnatal fiber type determination. *Stem Cells* 2010; **28**: 480–488.
13. Cenni V, Bertacchini J, Beretti F, Lattanzi G, Bavelloni A, Riccio M *et al.* Lamin A Ser404 is a nuclear target of Akt phosphorylation in C2C12 cells. *J Proteome Res* 2008; **7**: 4727–4735.
14. Capanni C, Del Coco R, Squarzoni S, Columbaro M, Mattioli E, Camozzi D *et al.* Prelamin A is involved in early steps of muscle differentiation. *Exp Cell Res* 2008; **314**: 3628–3637.
15. Hennekam RC. Hutchinson-Gilford progeria syndrome: review of the phenotype. *Am J Med Genet* 2006; **140**: 2603–2624.
16. Lombardi F, Gullotta F, Columbaro M, Filareto A, D'Adamo M, Vielle A *et al.* Compound heterozygosity for mutations in LMNA in a patient with a myopathic and lipodystrophic mandibuloacral dysplasia type A phenotype. *J Clin Endocrinol Metab* 2007; **92**: 4467–4471.
17. Garg A, Subramanyam L, Agarwal AK, Simha V, Levine B, D'Apice MR *et al.* Atypical progeroid syndrome due to heterozygous missense LMNA mutations. *J Clin Endocrinol Metab* 2009; **94**: 4971–4983.
18. Corrigan DP, Kuszczak D, Rusinol AE, Thewke DP, Hrycyna CA, Michaelis S *et al.* Prelamin A endoproteolytic processing *in vitro* by recombinant Zmpste24. *Biochem J* 2005; **387**(Part 1): 129–138.
19. Capanni C, Mattioli E, Columbaro M, Lucarelli E, Parnaik VK, Novelli G *et al.* Altered prelamin A processing is a common mechanism leading to lipodystrophy. *Hum Mol Genet* 2005; **14**: 1489–1502.
20. Lattanzi G, Columbaro M, Mattioli E, Cenni V, Camozzi D, Wehnert M *et al.* Pre-Lamin A processing is linked to heterochromatin organization. *J Cell Biochem* 2007; **102**: 1149–1159.
21. Capanni C, Del Coco R, Mattioli E, Camozzi D, Columbaro M, Schena E *et al.* Emerin-prelamin A interplay in human fibroblasts. *Biol Cell* 2009; **101**: 541–554.
22. Dominici S, Fiori V, Magnani M, Schena E, Capanni C, Camozzi D *et al.* Different prelamin A forms accumulate in human fibroblasts: a study in experimental models and progeria. *Eur J Histochem* 2009; **53**: 43–52.
23. Randles KN, Lam le T, Sewry CA, Puckelwartz M, Furling D, Wehnert M *et al.* Nesprins, but not sun proteins, switch isoforms at the nuclear envelope during muscle development. *Dev Dyn* 2010; **239**: 998–1009.
24. Crisp M, Liu Q, Roux K, Rattner JB, Shanahan C, Burke B *et al.* Coupling of the nucleus and cytoplasm: role of the LINC complex. *J Cell Biol* 2006; **172**: 41–53.
25. Liu Q, Pante N, Misteli T, Elsagga M, Crisp M, Hodzic D *et al.* Functional association of Sun1 with nuclear pore complexes. *J Cell Biol* 2007; **178**: 785–798.
26. Haque F, Mazzeo D, Patel JT, Smallwood DT, Ellis JA, Shanahan CM *et al.* Mammalian SUN protein interaction networks at the inner nuclear membrane and their role in laminopathy disease processes. *J Biol Chem* 2010; **285**: 3487–3498.
27. Xiong H, Rivero F, Euteneuer U, Mondal S, Mana-Capelli S, Larochelle D *et al.* Dictyostelium Sun-1 connects the centrosome to chromatin and ensures genome stability. *Traffic* 2008; **9**: 708–724.
28. Salpingidou G, Smertenko A, Hausmanowa-Petrucewicz I, Hussey PJ, Hutchison CJ. A novel role for the nuclear membrane protein emerin in association of the centrosome to the outer nuclear membrane. *J Cell Biol* 2007; **178**: 897–904.
29. Lattanzi G, Ognibene A, Sabatelli P, Capanni C, Toniolo D, Columbaro M *et al.* Emerin expression at the early stages of myogenic differentiation. *Differentiation* 2000; **66**: 208–217.
30. Lattanzi G, Cenni V, Marmiroli S, Capanni C, Mattioli E, Merlini L *et al.* Association of emerin with nuclear and cytoplasmic actin is regulated in differentiating myoblasts. *Biochem Biophys Res Commun* 2003; **303**: 764–770.
31. Hale CM, Shrestha AL, Khatau SB, Stewart-Hutchinson PJ, Hernandez L, Stewart CL *et al.* Dysfunctional connections between the nucleus and the actin and microtubule networks in laminopathic models. *Biophys J* 2008; **95**: 5462–5475.
32. Ostlund C, Folker ES, Choi JC, Gomes ER, Gundersen GG, Worman HJ. Dynamics and molecular interactions of linker of nucleoskeleton and cytoskeleton (LINC) complex proteins. *J Cell Sci* 2009; **122**(Part 22): 4099–4108.
33. Penkner AM, Fridkin A, Gloggnitzer J, Baudrimont A, Machacek T, Woglar A *et al.* Meiotic chromosome homology search involves modifications of the nuclear envelope protein Matefin/SUN-1. *Cell* 2009; **139**: 920–933.
34. Zhang J, Felder A, Liu Y, Guo LT, Lange S, Dalton ND *et al.* Nesprin 1 is critical for nuclear positioning and anchorage. *Hum Mol Genet* 2010; **19**: 329–341.
35. Zhang X, Lei K, Yuan X, Wu X, Zhuang Y, Xu T *et al.* SUN1/2 and Syne/Nesprin-1/2 complexes connect centrosome to the nucleus during neurogenesis and neuronal migration in mice. *Neuron* 2009; **64**: 173–187.
36. Gueneau L, Bertrand AT, Jais JP, Salih MA, Stojkovic T, Wehnert M *et al.* Mutations of the FHL1 gene cause Emery-Dreifuss muscular dystrophy. *Am J Hum Genet* 2009; **85**: 338–353.
37. Zhang Q, Bethmann C, Worth NF, Davies JD, Wasner C, Feuer A *et al.* Nesprin-1 and -2 are involved in the pathogenesis of Emery Dreifuss muscular dystrophy and are critical for nuclear envelope integrity. *Hum Mol Genet* 2007; **16**: 2816–2833.
38. Davies BS, Barnes II RH, Tu Y, Ren S, Andres DA, Spielmann HP *et al.* An accumulation of non-farnesylated prelamin A causes cardiomyopathy but not progeria. *Hum Mol Genet* 2010; **19**: 2682–2694.
39. Cenni V, Sabatelli P, Mattioli E, Marmiroli S, Capanni C, Ognibene A *et al.* Lamin A N-terminal phosphorylation is associated with myoblast activation: impairment in Emery-Dreifuss muscular dystrophy. *J Med Genet* 2005; **42**: 214–220.
40. Mattioli E, Columbaro M, Capanni C, Santi S, Maraldi NM, D'Apice MR *et al.* Drugs affecting prelamin A processing: effects on heterochromatin organization. *Exp Cell Res* 2008; **314**: 453–462.

Supplementary Information accompanies the paper on Cell Death and Differentiation website (http://www.nature.com/cdd)